UNIVERSITÀ
DEGLI STUDI
FIRENZE

FLORE
Repository istituzionale dell'Università degli Studi di Firenze

The Delineation of Paleo-Shorelines in the Lake Manyara Basin Using TerraSAR-X Data

Questa è la Versione finale referata (Post print/Accepted manuscript) della seguente pubblicazione:

Original Citation:

The Delineation of Paleo-Shorelines in the Lake Manyara Basin Using TerraSAR-X Data / Felix Bachofer; Geraldine Quénéhervé; Michael Maerker. - In: REMOTE SENSING. - ISSN 2072-4292. - STAMPA. - 6:(2014), pp. 2195-2212. [10.3390/rs6032195]

Availability:

This version is available at: 2158/911957 since:

Published version:

DOI: 10.3390/rs6032195

Terms of use:

Open Access

La pubblicazione è resa disponibile sotto le norme e i termini della licenza di deposito, secondo quanto stabilito dalla Policy per l'accesso aperto dell'Università degli Studi di Firenze (https://www.sba.unifi.it/upload/policy-oa-2016-1.pdf)

Publisher copyright claim:

(Article begins on next page)

05 May 2023

Remote Sens. **2014**, *6*, 2195-2212; doi:10.3390/rs6032195

OPEN ACCESS

remote sensing

ISSN 2072-4292

www.mdpi.com/journal/remotesensing

Article

The Delineation of Paleo-Shorelines in the Lake Manyara Basin Using TerraSAR-X Data

Felix Bachofer [1,*], Geraldine Queneherv é [1] and Michael M ärker [2,3]

[1] Institute of Geography, University of Tuebingen, Ruemelinstr, 19-23, D-72070 Tuebingen, Germany; E-Mail: geraldine.queneherve@uni-tuebingen.de

[2] Heidelberg Academy of Sciences and Humanities, Ruemelinstr, 19-23, D-72070 Tuebingen, Germany; E-Mail: michael.maerker@geographie.uni-tuebingen.de

[3] Earth Science Department, University of Florence, Via G. La Pira 4, I-50121 Florence, Italy

***** Author to whom correspondence should be addressed; E-Mail: felix.bachofer@uni-tuebingen.de; Tel.: +49-7071-29-77528; Fax: +49-7071-29-5378.

Received: 31 December 2013; in revised form: 18 February 2014 / Accepted: 27 February 2014 / Published: 10 March 2014

Abstract: The purpose of this paper is to describe the delineation of paleo-shorelines using high resolution microwave images and digital image processing tools, and with that to contribute to the understanding of the complex landscape evolution of the Lake Manyara Basin. The surroundings of Lake Manyara are the focus of several paleo-archeological investigations, since the location is close to Olduvai Gorge, where paleo-anthropological findings can be traced back to homo habilis. In the catchment of Lake Manyara two hominin-bearing sites (0.78 to 0.63 Ma), lots of vertebrate fossils and hand axes from different periods were found. Understanding the development and extent of the lake is crucial for understanding the regional paleo-environment of the Quaternary. Morphological structures of shorelines and terraces east of Lake Manyara were identified from TerraSAR-X StripMap images. By applying a Canny edge detector, linear features were extracted and revised for different image acquisitions using a contextual approach. Those features match literature and field references. A digital elevation model of the region was used to map the most distinct paleo-shorelines according to their elevation.

Keywords: Synthetic Aperture Radar (SAR); paleo-lake; TerraSAR-X; canny filter; edge detection

---

1. Introduction

Many authors have used lakes as indicators for climate and landscape changes in the Quaternary [1-6]. Lakes associated with the East African Rift System (EARS) respond in a quite sensitive way to tectonic and climatic changes [1]. Different studies therefore deal with the paleo-climate and the paleo-environment of this focus region [1,7–9]. Moreover, the direct and indirect influences of some of the EARS lakes on human evolution are intensively discussed. These lakes functioned as migration corridors or mixing barriers, and therefore contributed considerably to the development of biodiversity in the region [10].

The Lake Manyara Basin has been frequented by early hominins since the Early Middle Pleistocene. Hominin fragments of *Homo heidelbergensis* (see Figure 1), Acheulian material and a rich vertebrate fauna indicate the paleoanthropological importance of the region [11–13]. In addition, the vicinity to the hominin sites at Olduvai Gorge highlights the relevance of the Lake Manyara area in terms of paleo-landscape ecology and paleo-landscape development. Findings between Lake Manyara and the Engaruka Basin and in the vicinity of Makuyuni (see Figure 1) show that archaeological evidence is closely related to different paleolake stages [12,14]. One example is evidence from the Late Stone Age [14] (with radiocarbon dated findings from 9280 ± 60 y BP), which is related to a high lake level between 12,700 to 10,000 y BP [15,16].

Figure 1. The Lake Manyara Basin in Northern Tanzania.

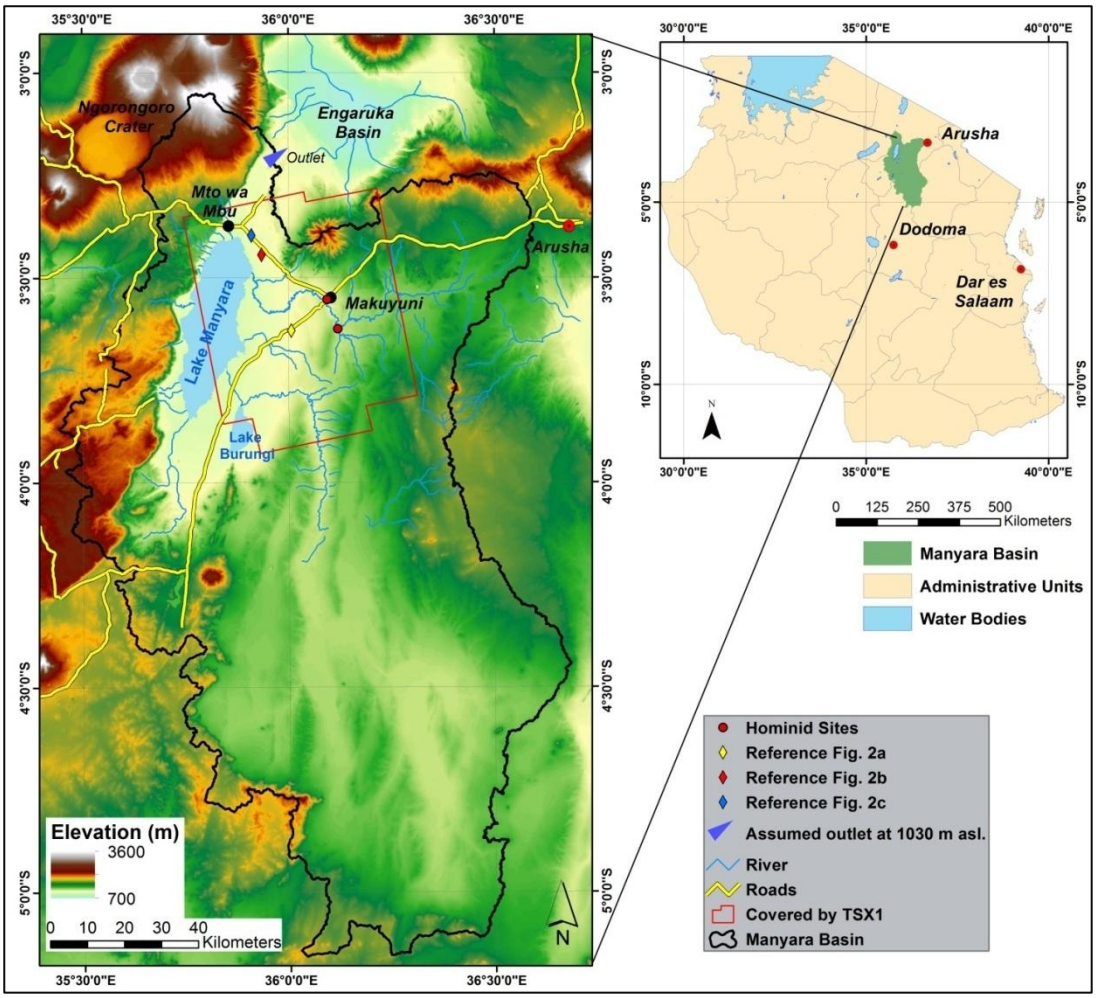

The Lake Manyara area is characterized by different lake levels that are related to specific paleo-shorelines, which appear mainly as terraces and beaches. These features and forms have been investigated only partly by detailed mapping and radiometric dating methods [17–19]. To the knowledge of the authors, a synoptic investigation of the spatial distribution of the paleolake shorelines, paleolake terraces and related features is not available. Thus, the objective of this study is to contribute to the understanding of the complex landscape evolution in the Lake Manyara area by delineating paleo-shorelines. The elevation of the shorelines in relation to the lowest outlet of the closed basin is also a focus point of the study. Because a delineation of the mentioned paleolake features was not feasible with optical remote sensing methods, backscatter intensity information from TerraSAR-X StripMap and ALOS PALSAR images were used. The morphological structures of shorelines and terraces east of Lake Manyara are characterized by high backscatter values, due to their geometric structure and texture. Linear features representing the paleo-shorelines were extracted from the intensity information of Synthetic Aperture Radar (SAR) images with a Canny edge detector and mapped in the study area. The results were linked to other studies of the Paleolake Manyara. A methodological approach in a similar context is not documented in the literature, to the knowledge of the authors.

In the last decades airborne and satellite remote sensing methodologies have been utilized increasingly for related tasks to detect paleo-landscape pattern, features and forms: Paleolakes on the Sinai Peninsula [20] were detected with IKONOS high resolution satellite imagery in combination with topographic analysis. Remote Sensing and topographical analysis were also used to delineate a paleolake in northern Darfur [21]. With Radarsat-1, Landsat ETM+ and a Shuttle Radar Topography Mission (SRTM), digital elevation model (DEM) paleo-shorelines and the paleolake highstand were identified in a megalake in Sudan [22]. SAR data was successfully applied in different studies for the mapping of subsurface geology and paleo-landscape [23,24]. Abdelsalam *et al.* [25] provide a thorough overview about the use of this methodology in arid regions. The integrated application of optical and microwave remote sensing and geospatial analysis also led to the successful delineation of buried paleo-drainages in Egypt, Sudan and Libya [26–28]. Single optical multispectral (e.g., ASTER) or high resolution (e.g., QuickBird) remote sensing data only allow the detection of the most prominent landscape features because of the spectral similarity of the covering material with its surroundings. Thus, in this study we utilize the TerraSAR-X sensor with its high resolution X-band images. This sensor offers the possibility to delineate distinct morphological structures due to the relation of backscatter intensity and geometry, texture and surface roughness [29,30].

Extracting line features is necessary for the delineation of paleo-shorelines. A general overview about line extraction methods is provided by Quackenbush [31]. Hellwich *et al.* [32] used a Markov Random Model and Bayesian classification for the extraction of linear objects from interferometric SAR data. Chanussot *et al.* [33] utilized a fuzzy fusion technique and a morphological line detector to extract a road network from multitemporal SAR images. Different Lee filters have been applied to derive linear features like coastlines from RADARSAT-1 and ERS-1 SAR data [34,35]. Using a Canny algorithm, Marghany [36] successfully delineated shoreline erosion from multitemporal SAR images.

2. Study Area and Paleolake Evidence

Lake Manyara (954 m a.s.l.) is located in an endorheic basin in the eastern branch of the EARS in northern Tanzania (Figure 1). The Manyara Basin is an asymmetrically shaped half graben, with a 200 to 600 m high escarpment in the west and a west dipping monocline in the east. The morphology of the landscape is strongly related to Quaternary volcanism and tectonic activity, which is still ongoing [36]. The basin is affected by minor *en echelon* step faults (NNE and E), whereas the lake sediments and the shorelines between Makuyuni and the lake are not disturbed by faulting [37–39]. The water supply originates from perennial springs and streams of the rift escarpment and from several seasonal drainages, of which the Makuyuni River and the Tarangire River are the largest. Today Lake Manyara is a shallow alkaline lake covering a varying area of up to approximately 550 km^2, with a maximum depth of 1.18 m, and can episodically dry out nearly completely [40]. The lowest possible outlet of the basin is located in the north of the lake along the main rift system, 78 to 80 m above today's lake level, and drains into the Engaruka Basin (Figure 1). The Tropical Rainfall Measurement Mission (TRMM) monthly Rainfall Estimate product 3B43 (V7) shows a bimodal rainfall pattern for the study area for the years 2000 to 2012, with a wet season from November to January and a second more intense wet season between March and May. The average annual precipitation ranges from 1200 mm at the escarpment to 700 mm at the plain east of the lake [41]. This results in a tropical semihumid vegetation cover with highland forests on the elevated areas west of the lake, and in a semiarid environment with bushed grassland east of the lake.

The oldest lacustrine strata within the Manyara Basin are known as the Manyara Beds and were first mentioned in 1942 [42]. They appear in the east of Lake Manyara and, based on sediments, define a maximum paleolake extent, approximately 140 m above today's lake surface. The Manyara Beds can be subdivided into a lacustrine grayish lower member (mudstones, siltstones, diatomite, marls and tuff) that was deposited between 1.3 to 0.98 Ma and 0.633 Ma, and a fluvial and terrestrial, up to 13 m thick, reddish-brown upper member (siltstones, mudstones, conglomerates and breccias) deposited between 0.633 Ma and 0.44 to 0.27 Ma. In most sections, the transition between both members is marked by a distinct tephra layer which was used for Ar^{40}/Ar^{39} dating [11,37,43]. The sections are best exposed close to the town of Makuyuni, where the sediments are partly overlain by a thin layer of Holocene soils and caliche and where big gully systems eroded into the savanna landscape.

The predominantly N-S aligned shorelines west of Lake Manyara vary from small beaches with a local relief of about 1 m to terraces that are several meters high. These terraces consist of up to three steps, indicating fluctuations of the distinct paleolake levels (Figure 2a). The terraces consist of conglomerates with different grain sizes up to 30 cm in diameter. The scarps are covered by coarse carbonates. The treads are sometimes vegetated by densely growing shrubs and small trees. Stromatolites and oncolites can be found along most of the ridges (Figure 2c). The areas between the shorelines are mostly covered by young carbonate rich soils, few are covered by carbonate gravel.

Figure 2. (**a**) Distinct paleo-shoreline (Lon. 36.006 °, Lat. −3.629 °); (**b**) Shoreline section (Lon. 35.909 °, Lat. −3.396 °); (**c**) Stromatolites and oncolites (Lon. 35.934 °, Lat. −3.444 °); Compare with Figure 1.

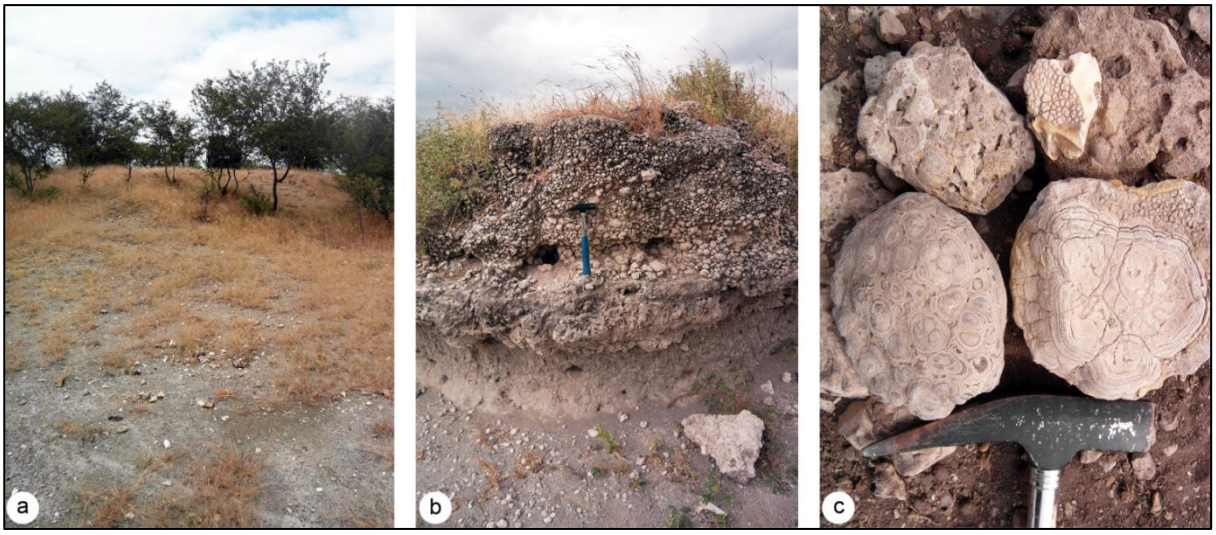

Several authors mention younger evidence of different paleolake phases than the lower member of the Manyara Beds. At the beginning of the 20th century, former shorelines and beaches up to 40 m above today's lake level were detected [44,45]. A complete series of beach terraces was found and identified as different shorelines of pluvial periods [46]. A first systematic documentation of shorelines was published in 1975 for the Lake Manyara and the Engaruka Basin [17]. The authors found eight main terraces and several beaches in the Lake Manyara Basin and mapped them without taking elevation information in the vicinity of the road leading from Makuyuni to the southern part of the lake. Another study identified four different lake levels about 6 m, 21 m, 43 to 52 m and 82 m above the current level, respectively, during field visits. The highest level also marks the threshold of a lowest possible outlet to the Engaruka and Natron-Magadi Basin [19]. These terraces have not been mapped for the whole basin yet, and the description of their location remains vague.

Other research has focused on oncolites and stromatolites, which are closely connected to flat tidal environments and therefore, have been documented as evidence for paleo-shorelines [18,47]. In an analysis of stromatolites from the northwestern area of today's lake extent close to the town of Mto Wa Mbu (Figure 1) [18], late Pleistocene and Holocene stromatolites collected on a distinct level of 20 m above today's lake level were dated by ^{14}C and Th/U series. Results showed humid periods with high lake levels for 22,000 y BP (increased water residence time, nutrient enrichment), 27,000 to 23,000 y BP (stable hydrological conditions with diluted fresh water), 35,000 to 32,000 y BP, 90,000 y BP, and an uncertain age of about 140,000 y BP [18,48]. Other research groups dated the humid period between 27,500 and 26,000 y BP, and an even younger high stand between 12,700 to 10,000 y BP by diatom analysis of two drilling cores from Lake Manyara [15,16]. All radiocarbon ages corroborate other studies of lake level fluctuations along the EARS. For the Nakuru-Elmenteita and the Naivasha Basin high lake level stands were postulated for the periods 146,000 to 73,300 y BP and 15,200 to 9600 y BP [1,49]. Trauth *et al.* [7] studied the nearby Ol Njorowa Gorge where they detected high level stands at 146,000 to 141,000 y BP and ca. 93,000 to 89,000 y BP (amongst other time intervals for the Upper Pleistocene). Garcin *et al.* [50] suggested high paleolake levels for Lake Suguta

for the periods 16,500 to 15,000 y BP, a high stand at 12,800 y BP and a high lake level from 11,800 y BP to 8500 y BP. For the Lake Natron-Magadi Basin north of Lake Manyara ages for stromatolites and related shorelines (ca. 240,000 y BP, 135,000 ± 10,000 y BP and from 12,000 to 10,000 y BP) have been found to differ from the ages of stromatolites of the Lake Manyara Basin, but agree with the ages of the other lake systems mentioned before, and the ages of the drilling cores of Lake Manyara [3,48]. The comparison of stromatolite ages in East African lake systems may involve a methodological problem, because the encrusting benthic microbial communities react very sensitively to changes in water chemistry and hydrological conditions. Therefore, stromatolites do not necessarily indicate all paleolake levels and radiometric dating and interpretation should not focus solely on these materials [18]. Trauth *et al.* [7] provide a synoptic view on East African climate change and lake systems for the last 175,000 y.

3. Methodology

3.1. SAR Processing

Six TerraSAR-X (TSX1) (~9.65 GHz; X-band) StripMap and two ALOS PALSAR (~1.27 GHz; L-band) scenes for different dates were acquired for the delineation of the paleo-shorelines (Table 1). All scenes were ordered in SLC format. The precipitation induced soil moisture increases the backscattering intensity for the soil covered areas and reduces the ability to discriminate the relevant structures of the paleo-shorelines [29,30]. Because soil moisture information with a sufficient resolution was not available, TRMM daily Rainfall Estimate product 3B42 (V7) was used to examine the days preceding the acquisition dates for relevant precipitation [41]. Relevant precipitation was measured only for the days prior to the 2013-01-15 TSX1 scene. Visual inspection confirmed a reduced contrast between the probable paleo-shorelines and their surroundings for the 2013-01-15 scene, but the most distinctive structures were still recognizable and therefore, the scene was not excluded from further processing.

Table 1. List of SAR images of the study area. Inc. Ang., incident angle at scene center; Pol., polarization; deg., degrees; Asc., Ascending.

Nr.	Sensor	Mode	Date	Time (UTC)	Orbit	Inc. Ang. (deg.)	Pol.
1	TSX1	StripMap	2011-09-08	15:46:08	Asc.	26.3 °	HH
2	TSX1	StripMap	2011-08-28	15:46:08	Asc.	26.3 °	HH
3	TSX1	StripMap	2011-09-13	15:54:39	Asc.	44.4 °	HH
4	TSX1	StripMap	2011-09-02	15:54:39	Asc.	44.4 °	HH
5	TSX1	StripMap	2012-12-24	15:46:10	Asc.	25.8 °	HH/HV
6	TSX1	StripMap	2013-01-15	15:46:08	Asc.	24.5 °	HH/HV
7	ALOS PALSAR	Fine Beam	2008-05-24	20:22:03	Asc.	38.8 °	HH/HV
8	ALOS PALSAR	Fine Beam	2010-07-15	20:25:27	Asc.	38.8 °	HH/HV

The TSX1 and ALOS PALSAR scenes were radiometrically calibrated to sigma naught (σ^0) by applying a correction factor to the radar brightness product (β^0). Further, radiometric normalization was applied to correct for topography using a SRTM-X DEM and the local incident angle resulting in gamma naught (γ^0) [51,52]. Multilooking was applied to all scenes and they were terrain corrected. To

reduce speckle effects in the images and to pronounce morphological features they were filtered using a Lee filter [53]. Whereas the paleo-shorelines are hardly noticeable in optical remote sensing images, they are highlighted by their intense backscatter in TSX1 (Figure 3a,b). The resulting images were resampled to 3 m pixel resolution for TSX1 and to 20 m resolution for PALSAR images. The inter-scene spatial conformity is important for the following image processing steps. The high accuracy of orbital parameters of TSX1 data makes a further co-registration unnecessary [54]. The co-registration from ALOS PALSAR to the TSX1 scenes appeared insufficient for the purposes of this study, due to the different spatial resolution. Since the PALSAR images also did not show additional information of the relevant structures they were excluded from further processing.

Figure 3. Example of the workflow for a small area; (**a**) Optical reference image; (**b**) TSX1 image (13 September 2011); (**c**) Result of the Canny edge detector (background: transparent TSX1 image); (**d**) Results of shoreline extraction after post-processing.

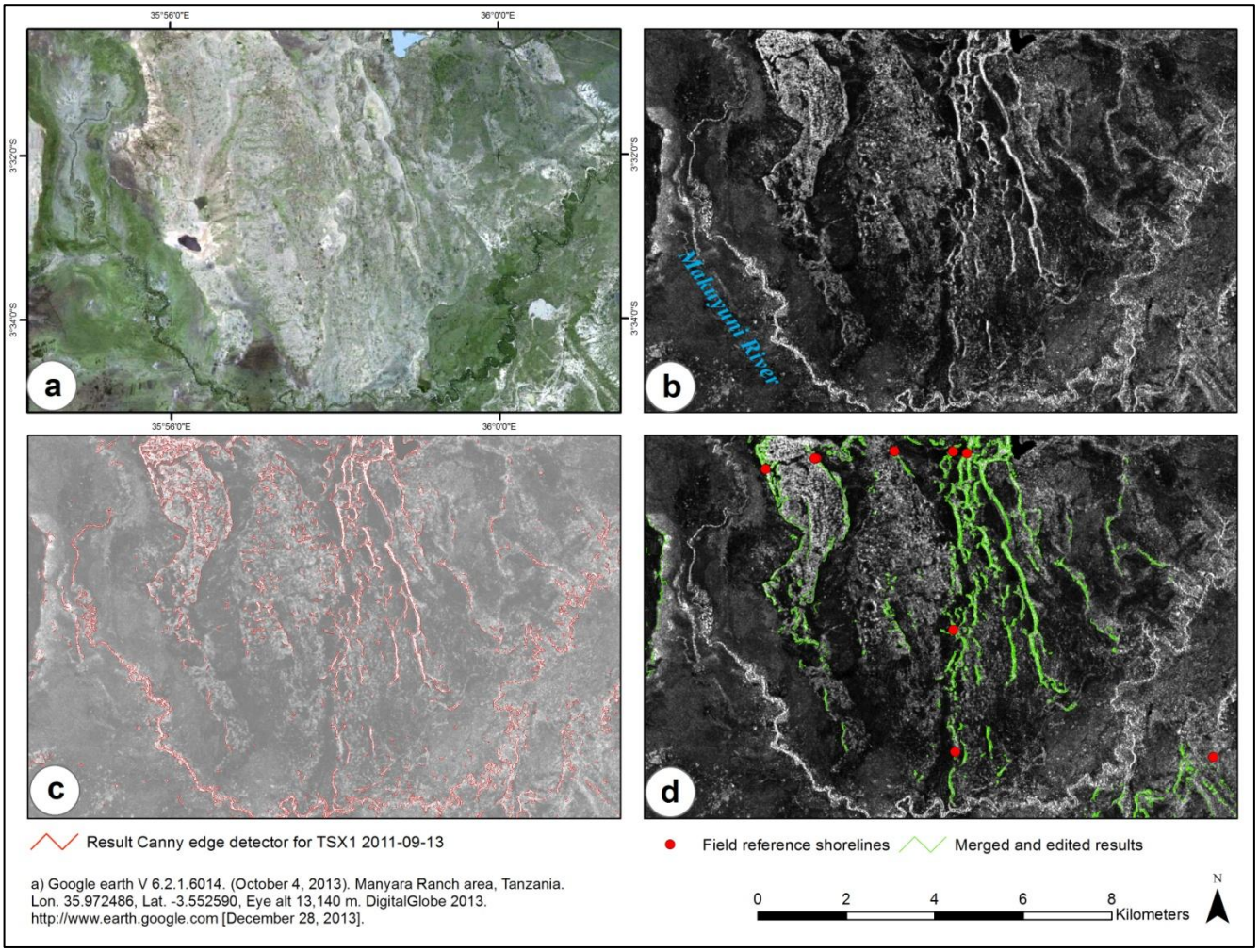

3.2. Filtering and Further Image Processing

The speckle effect makes the detection of linear features in SAR images more difficult than in optical images [34]. With the Lee filter (5 × 5) the speckle noise could be reduced while the contrast of the linear features could be preserved. The linear structures of the images were extracted from the derived image products using a Canny edge detector from the Python scikit-image module for the

SciPy library [55]. Edge detectors in general reduce the information content of an image to the structural information about objects [56]. To enhance the results of the edge detector and to be able to use similar weighting parameters for the Canny filter, all images were contrast stretched and normalized to a range from 0 to 1. The Canny procedure first applies a Gaussian filter to reduce noise in the original image. Subsequently, the strength of value gradients between the image pixels is computed by applying a directional Sobel operator. In addition, the direction of edges is approximated to vertical, horizontal and $\pm 45°$ directions. This is followed by a nonmaximum suppression, which suppresses all values along the magnitude of gradients that are not considered to be an edge to zero. Finally hysteresis thresholding is applied resulting in a lower and an upper threshold to reduce streaking effects. To achieve a good trade-off between the detection of a maximum of linear features including small beaches and the suppression of unnecessary features, the weighting parameters for the standard deviation of the Gaussian filter had to be adjusted for each scene. For hysteresis thresholding good results could be achieved with a ratio of high to low threshold of 3.5:1 (Figure 3c). The results are binary raster files with the value one representing linear features.

Morphological image processing was applied using a closing operator (dilation & erosion) to close gaps between detected lines (adjacent pixel elements) [31]. The resulting raster maps were added up to a single raster layer where structures detected in multiple scenes hold values greater than one. Only those structures were considered for further processing. An opening procedure (erosion & dilation) was applied to minimize the number of artifacts [31]. The remaining structures were reduced to their skeletons and converted into vector format. Contextual information was used to exclude features like roads and river beds (Figure 3c,d), as well as forests of the Lake Manyara National Park to the north and west of the lake, and a forested flood plain north of Lake Burungi. Many linear structures were identified on the slopes of the volcanic cone of the Essimingor northeast of the lake. The radial valleys of the volcano result in linear structures similar to shorelines (Figure 4). The western and northwestern slopes of Essimingor may have been reached by the lake during a high stand but other lines on the volcanic cone were deleted. Some of the areas between the shorelines west of Essimingor are covered by rough gravel and resulted in some artifacts that were verified in the field and removed by manual editing (Figure 3c,d; compare northwestern parts of the displayed areas).

3.3. Lake Level

SRTM-X DEM (30 m) data covers nearly the whole Manyara Basin and was seamlessly combined with a SRTM-3 DEM (90 m) to achieve coverage of the whole basin. A morphology preserving multidirectional Lee Filter for noise and artifact reduction was applied [53]. High accuracy ICESat altimetry data from 15 overpasses over Lake Manyara between 2003 and 2009 were processed to calculate a mean lake level of 954.25 m (EGM96, standard deviation of 35 cm) [57]. The SRTM-X lake level was adjusted to this height. SRTM data as well as most studies used a height of 960 m for the lake surface and as base height for relative measurements for the elevation of shorelines [18,19]. The identified paleo-shoreline features were converted to points and the corresponding heights where extracted from the DEM. The different levels of the shorelines can be traced and distinguished on the eastern side of Lake Manyara (Figure 4). The derived elevation values from SRTM-X are within a relative vertical accuracy of ± 6 m [58,59].

Figure 4. Identified shorelines (generalized for mapping issues) and field reference data from June 2013.

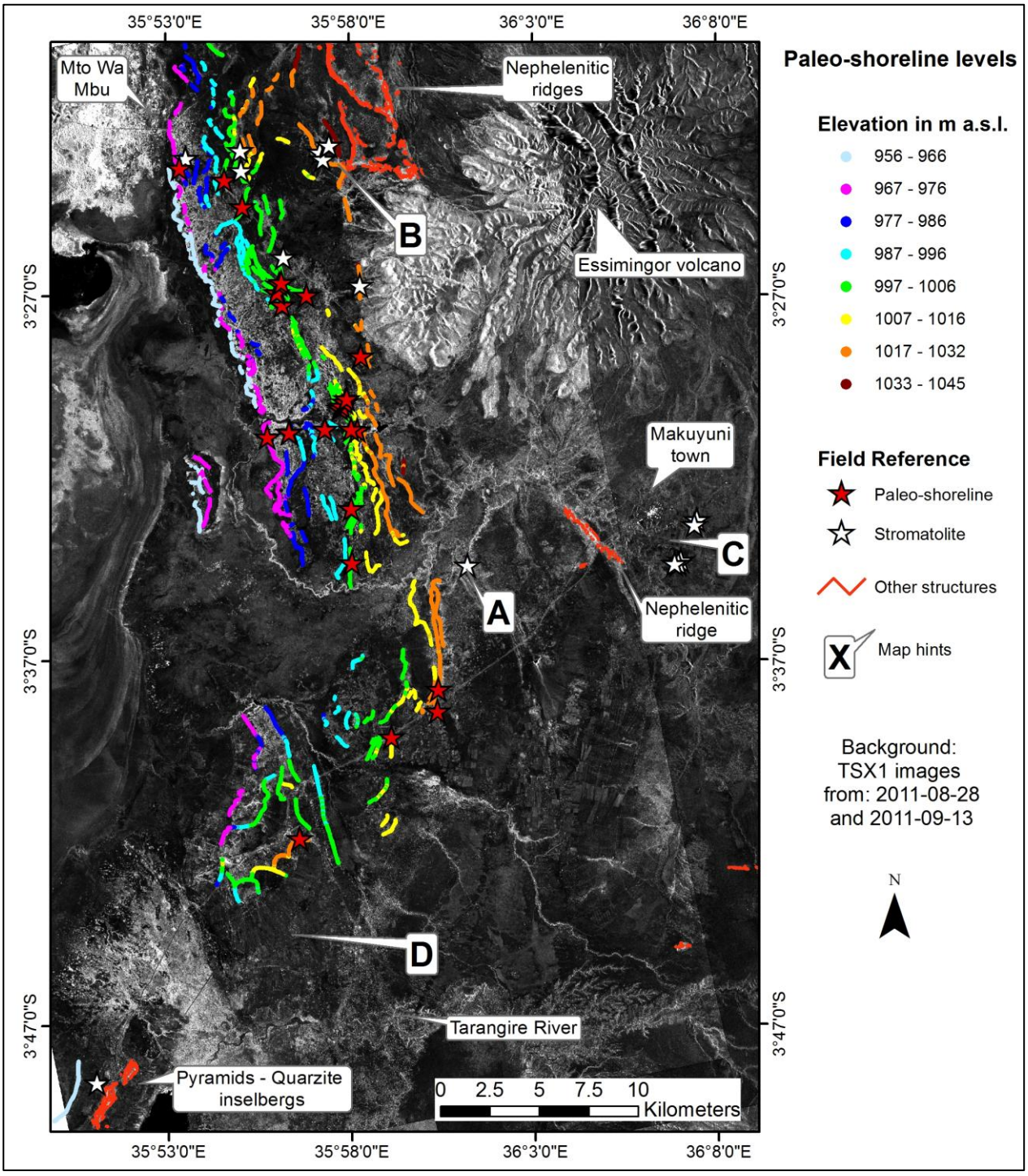

4. Results and Discussion

Different sources were used for the validation of the results. Two studies are applicable as reference from the published literature. Eight main terraces and several beaches were found and mapped up to an elevation of 1,115 m a.s.l. within the vicinity of the road leading from Makuyuni in SE direction by Keller *et al.* [17]. Four different lake levels were identified in the field but not mapped by Somi [19].

As further reference for this study, 25 paleo-shorelines and the occurrence of stromatolites (14) east of Lake Manyara were mapped with GPS points in the field during surveys in 2012 and 2013 (Figure 4).

A dense occurrence of shorelines can be seen northeast of the lake. Distinct levels of paleo-shorelines start from about 6 m to 80 m above today's lake level, some features even a few meters higher. The most frequent elevation for the occurrence of shorelines is between 1002 m and 1008 m a.s.l. (48 to 54 m above today's lake level, Figures 5 and 6). The large number of linear lacustrine features across the entire range of elevations is indicative of nearly-continuous lake level evidence by transgression and regression periods. The Makuyuni River, draining from Makuyuni into the Lake Manyara, later eroded some of the paleo-shorelines and disturbed their original distribution. The morphology of ancient shorelines is also eroded or disturbed by the Tarangire River, draining the southeastern part of the Lake Manyara Basin. The proposed method identified 24 of 25 paleo-shorelines marked by GPS points during field survey. Further, the paleolake level 2 to 6 described by Keller *et al.* [17] were delineated. The geometry of paleolake stage level 1 closest to the lake is not well enough defined for high backscatter signals. The paleolake level 7 and 8 [17] are located on elevations up to 1115 m a.s.l. and far above the lowest possible outlet into the Engaruka Basin. They coincide with the Manyara Beds, but do not agree well with findings of other studies [11,22].

No faulting for the identified shorelines can be stated, which coincides with [37–39]. Since the shorelines are in a parallel sequence and only interrupted by fluvial processes tectonic activity has not, or only marginally, affected the absolute elevations of the detected paleo-shorelines since the formation of these structures. This can be maintained at least for the shorelines in the east of the central lake and to the northeast and north of the lake. In the southeast of the lake, insufficient shorelines remain to make a corresponding statement.

Figure 5. Histogram of paleo-shoreline height level distribution. Yellow bars indicate the lake levels visualized in Figure 6.

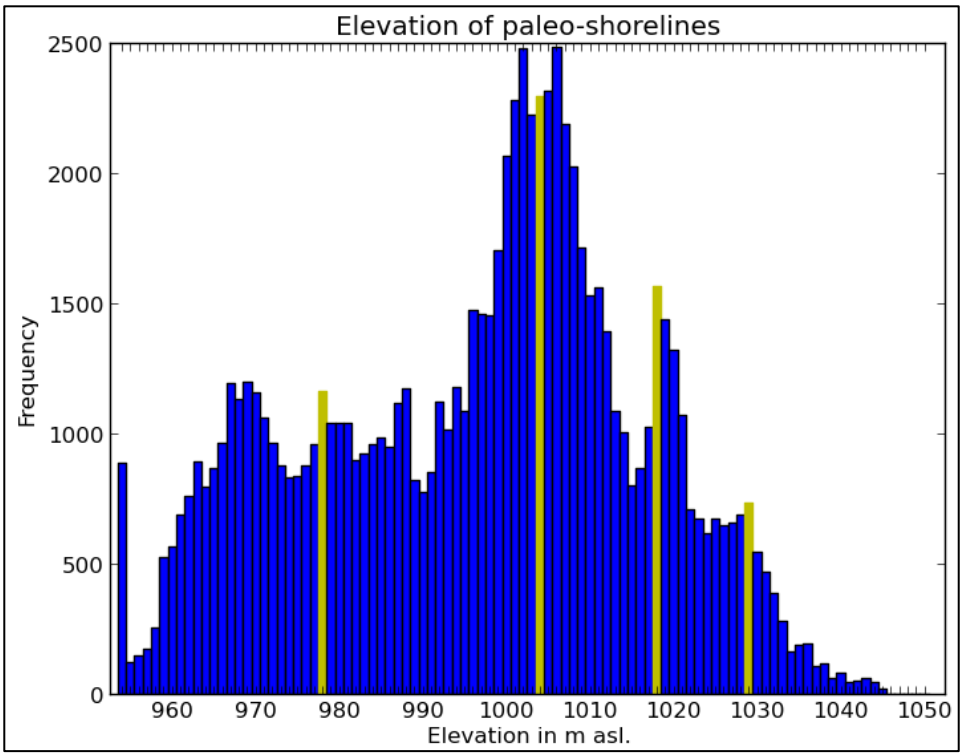

Figure 6. Different paleolake stages.

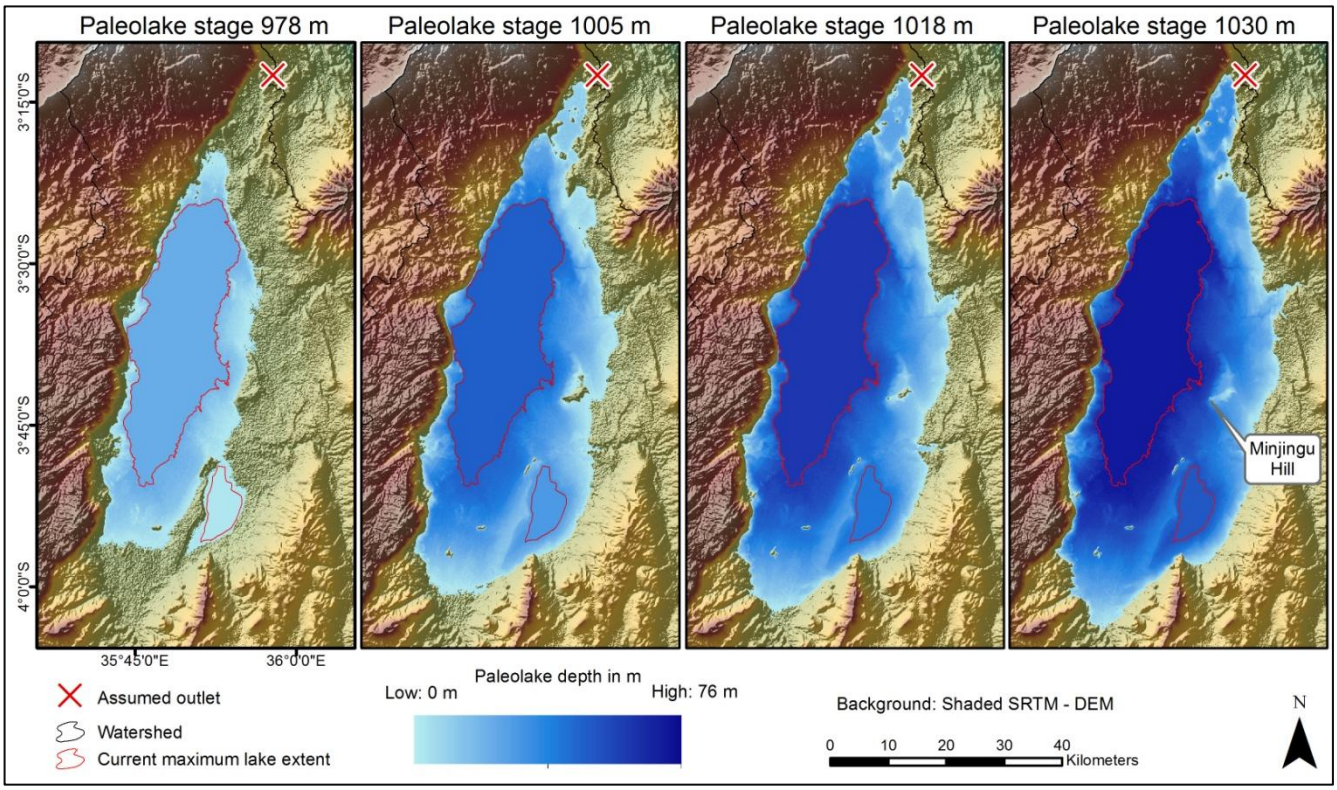

Some structures in the southeast of Lake Manyara that were mapped as smaller "beach ridges" [17] and are marked with "D" (Figure 4) could not be identified by TSX1 analysis. Because the beach ridges are not described by Keller *et al.* [17] and no field observations are available for this region we can only assume that they are too small to be detected by our analysis, or that their geometry is not well defined. Paleo-shorelines north and west of the inselbergs "Pyramids" were recognized.

Some prominent shorelines at the level of 1030 m to 1036 m a.s.l., reported by Somi [19], could not be identified by our method or during field surveys. Because their position is not described clearly and the structures are not mapped, they might be located outside the area covered by the SAR images. Alternatively, the structures might be hidden by dense trees and shrub vegetation of the Tarangire National Park so that backscatter signals fail to delineate distinct features. In addition, the PALSAR L-Band scenes could not identify these shorelines. In contrast, structures mentioned by Somi [19] close to Mto Wa Mbu and in the northeast of the Lake were clearly identified.

Linear features other than paleo-shorelines were also identified by the implemented method. These had to be reclassified using existing maps and field reference data. The structures are nephelenitic ridges north of Essimingor and west of Makuyuni, which resulted from volcanic activity, and some quartzite inselbergs southeast of Lake Manyara (Figure 4). The location marked with "A" (Figure 4) shows a section incised by the Makuyuni River, where stromatolites were found during field survey. Corresponding paleo-shorelines could not be identified in the field or by image analysis. It is likely that they belong to the older lake sediments of the Lower Manyara Beds ("C", Figure 4) close to Makuyuni, which have a radiometric age older than 0.633 Ma [11]. The Lower Manyara Beds are not the focus of this study, because they do not form distinct shorelines on the surface, because their age

exceeds the radiometric age of the paleo-shorelines, and because they have been found so far only in the surroundings of Makuyuni.

As mentioned before, we identified structures located up to 80 m above today's lake level. This is interesting because the threshold of the first possible outlet of the Manyara Basin is at about 1032 m and leads into the Engaruka and to the Natron-Magadi Basin in the north. Some authors assume that the lake level did not reach this elevation [18], others assume an even higher level above 1050 m a.s.l. [15,42], and other authors expect the maximum level of the shorelines to be around the level of the lowest possible outlet [19]. With the results from this study and the evidence of the maximum shoreline heights from field survey conducted in this study, we agree with the latter authors. The location marked with a "B" (Figure 4) illustrates the abundance of stromatolites on linear features. In this unique situation, stromatolites and oncolites are sparsely distributed on a mafic ridge and not on a well-defined shoreline. They occur four meters above the threshold for today's outflow, which can be explained by tectonic processes or an incision of the outlet from the Manyara Basin to the Engaruka Basin. By tracing these maximum lacustrine sediments to the south along the slopes of the Essimingor volcano, linear structures continue until a reference point confirms a shoreline. Directly beneath the slopes of Essimingor the paleo-shoreline might be covered by material from the talus of the volcano, like it is the case for the shorelines west of the lake at the escarpment [19]. The ridges to the east of "B" (Figure 4) are absent of lacustrine carbonate.

The histogram of the paleo-shoreline height levels (Figure 5) shows a peak at the current lake level, followed by a gap and then a steady occurrence from 960 m a.s.l. to 1040 m a.s.l. The continuous distribution of shorelines within this range indicates fluctuating lake levels. The peaks in the histogram at 970 m, 978 m, 1002 m to 1008 m, 1018 m and 1030 m depict more steady paleo-environmental conditions. For the paleolake stages marked with yellow bars in Figure 5 (24 m, 51 m, 64 m and 78 m above the current lake level) the lake extent is illustrated in Figure 6. For those paleolake levels the lake volume and the corresponding surface area were calculated (Table 2).

Table 2. Statistical evaluation of Lake Manyara paleolake stages.

Lake level	Lake Depth	Lake Volume	Surface Area
Today (954 m)	1.18 m	~0.5 km^3 *	610 km^2 (including Lake Burungi)
978 m	24 m (above today)	20.0 km^3	1152 km^2
1005 m	51 m (above today)	59.6 km^3	1757 km^2
1018 m	64 m (above today)	83.6 km^3	1932 km^2
1030 m	76 m (above today)	107.6 km^3	2062 km^2

* A bathymetric survey showed a maximum depth of 1.18 m and an average depth of 0.81 m for Lake Manyara, without Lake Burungi [23].

The lake volume and the lake surface area increase drastically with higher lake levels (Figure 6, Table 2), which is caused by the flat plain in the north, south and west of the lake. Due to the strong increase in surface, the Paleolake Manyara must have been very sensitive to climatic changes in this high temperature environment. Changes in precipitation and temperature are strongly correlated with evapotranspiration rates [17]. On one hand, this explains the amount of paleo-shorelines, and on the other hand, it suggests that Lake Manyara passed through several transgression and regression phases.

Further paleolake evidence can be confirmed for Minjingu Hill, a small inselberg five kilometers east of Lake Manyara (Figure 6). The topographic analysis shows that, even with a high stand of the lake at 1030 m (close to the height of the outlet), the hill is still not covered by water, and that very shallow waters emerge to the east of it. The hill served as a platform for cormorants which produced large quantities of guano; today, phosphate is mined in this area [17,19,60].

Overall, the detection of paleo-shorelines using the intensity information of TSX1 data was successful. The parallel orientation of the paleo-shorelines in the Lake Manyara Basin relative to the flight direction of the satellite causes a strong backscatter signal. The proposed workflow of speckle filtering to remove noise, the Canny algorithm to identify linear features, and morphological operators to extract the linear structures from the SAR images did perform well for the purpose of this study. The mapping approach is semi-automated because contextual information was necessary to remove or identify other linear features like roads, river beds and volcanic ridges. The transferability of the methodological approach is therefore limited by the availability of additional sources about other linear structures in the respective study area. Assessing the accuracy of the approach is challenging because the collection of reference points in remote areas like some parts of the Manyara Basin is difficult. Single reference points allow verifying whether a paleo-shoreline could be detected by the proposed method. To assess the completeness of the morphology of the detected paleo-shorelines, the mapping of distinct sections with multiple GPS points or kinematic measurements in the field would have been an advantage. With the field reference and literature sources [17,19], we can provide a qualitative assessment that our approach yielded good mapping results of the paleo-shorelines in the Lake Manyara Basin.

5. Conclusions

Our study shows that microwave remote sensing, image processing and topographic analysis can be combined successfully to identify and map paleo-shorelines in the Lake Manyara area, and can thereby contribute to the spatial reconstruction of paleo-environments. The endorheic Lake Manyara Basin in the eastern branch of the East African Rift System underwent different transgression and regression phases. A distinct morphologic feature of these lake fluctuations is paleo-shorelines in the form of terraces and beaches on different elevation levels across the landscape. Stromatolites of a distinct paleo-shoreline level have been radiometrically dated previously [17], leading to different conclusions about the amplitude of this fluctuations and the location of these shorelines [15,17–19,42]. In this study, we used the backscattering information of the paleo-shoreline geometry, roughness and surface cover to describe their spatial distribution. We utilized image processing methods to extract linear features and validated the results with reference data from field surveys and from literature review. In combination with a refined digital elevation model, the paleo-shoreline features served as base for the reconstruction of the paleolake stages of Lake Manyara. Some prominent paleolake levels were extracted and their spatial extent mapped (Figure 5). A maximum lake level was identified slightly above the lowest possible outlet in the north, which indicates a possible overspill into the neighboring Engaruka Basin and into the Natron-Magadi Basin in the north. The reconstructed lake level seems reasonable in the context of other research conducted in the Lake Manyara Basin. To assess the dynamics of the different transgression and regression phases and the corresponding shorelines more

detailed, additional radiometric datings are necessary. Further research is needed to help understand the emergence of the so called Lower Manyara Beds, which was not addressed in this study.

Acknowledgments

This study was financed by the Heidelberg Academy of Sciences and Humanities research center: "The Role of Culture in Early Expansions of Humans" (ROCEEH). The data used in this work were acquired as part of the activities of NASA's Science Mission Directorate, and are archived and distributed by the Goddard Earth Sciences (GES) Data and Information Services Center (DISC). We would like to thank the DLR and the German Remote Sensing Data Center (DFS) for providing the TerraSAR-X and the SRTM/X-SAR data. We acknowledge support by Deutsche Forschungsgemeinschaft and Open Access Publishing Fund of Tuebingen University.

Author Contributions

Felix Bachofer was responsible for the research design, the processing of the SAR images and the digital image analysis. All authors contributed to the collection of ground reference data during three field campaigns from 2011 to 2013. Felix Bachofer wrote the initial manuscript with significant input of Geraldine Quénéhervé and Michael Märker on the paleo-environmental context and the interpretation of the results.

Conflicts of Interest

The authors declare no conflict of interest.

References

1. Bergner, A.G.N.; Strecker, M.R.; Trauth, M.H.; Deino, A.; Gasse, F.; Blisniuk, P.; Dühnforth, M. Tectonic and climatic control on evolution of rift lakes in the Central Kenya Rift, East Africa. *Quatern. Sci. Rev.* **2009**, *28*, 2804–2816.
2. Washbourn, C.K. Lake levels and quaternary climates in the Eastern Rift valley of Kenya. *Nature* **1967**, *216*, 672–673.
3. Casanova, J. Stromatolites from the East African Rift: A synopsis. In *Phanerozoic Stromatolites II*; Bertrand-Sarfati, J., Monty, C., Eds.; Springer: Dordrecht, The Netherlands, 1994; pp. 193–226.
4. Burrough, S.L.; Thomas, D.S.G.; Bailey, R.M. Mega-lake in the Kalahari: A late Pleistocene record of the Palaeolake Makgadikgadi system. *Quatern. Sci. Rev.* **2009**, *28*, 1392–1411.
5. Olaka, L.; Odada, E.; Trauth, M.; Olago, D. The sensitivity of East African Rift lakes to climate fluctuations. *J. Paleolimnol.* **2010**, *44*, 629–644.
6. Bergner, A.G.N.; Trauth, M.H. Comparison of the hydrological and hydrochemical evolution of Lake Naivasha (Kenya) during three highstands between 175 and 60 kyr BP. *Palaeogeogr. Palaeoclimatol. Palaeoecol.* **2004**, *215*, 17–36.
7. Trauth, M.H.; Deino, A.L.; Bergner, A.G.N.; Strecker, M.R. East African climate change and orbital forcing during the last 175 kyr BP. *Earth Planet. Sci. Lett.* **2003**, *206*, 297–313.

8. Barker, P.; Gasse, F. New evidence for a reduced water balance in East Africa during the Last Glacial Maximum: Implication for model-data comparison. *Quatern. Sci. Rev.* **2003**, *22*, 823–837.
9. Schüler, L.; Hemp, A.; Zech, W.; Behling, H. Vegetation, climate and fire-dynamics in East Africa inferred from the Maundi Crater pollen record from Mt Kilimanjaro during the last glacial-interglacial cycle. *Quatern. Sci. Rev.* **2012**, *39*, 1–13.
10. Trauth, M.H.; Maslin, M.A.; Deino, A.L.; Junginger, A.; Lesoloyia, M.; Odada, E.O.; Olago, D.O.; Olaka, L.A.; Strecker, M.R.; Tiedemann, R. Human evolution in a variable environment: The amplifier lakes of Eastern Africa. *Quatern. Sci. Rev.* **2010**, *29*, 2981–2988.
11. Frost, S.R.; Schwartz, H.L.; Giemsch, L.; Morgan, L.E.; Renne, P.R.; Wildgoose, M.; Saanane, C.; Schrenk, F.; Harvati, K. Refined age estimates and Paleoanthropological investigation of the Manyara Beds, Tanzania. *J. Anthropol. Sci.* **2012**, *90*, 1–12.
12. Kaiser, T.M.; Seiffert, C.; Hertler, C.; Fiedler, L.; Schwartz, H.L.; Frost, S.R.; Giemsch, L.; Bernor, R.L.; Wolf, D.; Semprebon, G.; *et al.* Makuyuni, a new lower Palaeolithic hominid site in Tanzania. *Mitteilungen Hamburgisches Zool. Museum Inst.* **2010**, *106*, 69–110.
13. Wolf, D.; Nelson, S.V.; Schwartz, H.L.; Semprebon, G.M.; Kaiser, T.M.; Bernor, R.L. Taxonomy and paleoecology of the Pleistocene Equidae from Makuyuni, Northern Tanzania. *Palaeodiversity* **2010**, *3*, 249–269.
14. Seitsonen, O. Archaeological research in the Northern Lake Manyara Basin, Tanzania, 2003–2004. *Azania: J. Br. Inst. Eastern Afr.* **2006**, *41*, 41–67.
15. Holdship, S.A. *The Paleolimnology of Lake Manyara, Tanzania: A Diatom Analysis of a 56 m Sediment Core*; Duke University: Durham, NC, USA, 1976.
16. Barker, P.A. *Diatoms as Palaeolimnological Indicators: A Reconstruction of Late Quaternary Environments in Two East African Salt Lakes*; Loughborough University of Technology: Loughborough, UK, 1990.
17. Keller, C.M.; Hansen, C.; Alexander, C.S. Archaeology and paleoenvironments in the Manyara and Engaruka Basins, Northern Tanzania. *Geogr. Rev.* **1975**, *65*, 364–376.
18. Casanova, J.; Hillaire-Marcel, C. Chronology and paleohydrology of late Quaternary high lake levels in the Manyara Basin (Tanzania) from isotopic data (18O, 13C, 14C, ThU) on fossil stromatolites. *Quatern. Res.* **1992**, *38*, 205–226.
19. Somi, E.J. *Paleoenvironmental Changes in Central and Coastal Tanzania During the Upper Cenozoic: Magnetostratigraphy, Sedimentary Records and Shorelevel Changes*; Paleogeophysics & Geodynamics, Department of Geology and Geochemistry, University of Stockholm: Stockholm, Sweden, 1993.
20. Gaber, A.; Ghoneim, E.; Khalaf, F.; El-Baz, F. Delineation of paleolakes in the Sinai Peninsula, Egypt, using remote sensing and GIS. *J. Arid Environ.* **2009**, *73*, 127–134.
21. Elmahdy, S.I. Hydromorphological mapping and analysis for characterizing darfur paleolake, NW Sudan using remote sensing and GIS. *Int. J. Geosci.* **2012**, *2012*, 25–36.
22. Ghoneim, E.; El-Baz, F. The application of radar topographic data to mapping of a mega-paleodrainage in the Eastern Sahara. *J. Arid Environ.* **2007**, *69*, 658–675.
23. Dabbagh, A.E.; Al-Hinai, K.G.; Asif Khan, M. Detection of sand-covered geologic features in the Arabian Peninsula using SIR-C/X-SAR data. *Remote Sens. Environ.* **1997**, *59*, 375–382.

24. Schaber, G.G.; McCauley, J.F.; Breed, C.S. The use of multifrequency and polarimetric SIR-C/X-SAR data in geologic studies of Bir Safsaf, Egypt. *Remote Sens. Environ.* **1997**, *59*, 337–363.
25. Abdelsalam, M.G.; Robinson, C.; El-Baz, F.; Stern, R.J. Application of orbital imaging radar for geologic studies in arid regions: The Saharan Testimony. *Photogram. Eng. Remote Sens.* **2000**, *66*, 717–726.
26. Ghoneim, E.; El-Baz, F. DEM-optical-radar data integration for palaeohydrological mapping in the northern Darfur, Sudan: Implication for groundwater exploration. *Int. J. Remote Sens.* **2007**, *28*, 5001–5018.
27. Rahman, M.M.; Tetuko Sri Sumantyo, J.; Sadek, M.F. Microwave and optical image fusion for surface and sub-surface feature mapping in Eastern Sahara. *Int. J. Remote Sens.* **2010**, *31*, 5465–5480.
28. Ghoneim, E.; Benedetti, M.; El-Baz, F. An integrated remote sensing and GIS analysis of the Kufrah Paleoriver, Eastern Sahara. *Geomorphology* **2012**, *139–140*, 242–257.
29. Zribi, M.; Kotti, F.; Lili-Chabaane, Z.; Baghdadi, N.; Ben Issa, N.; Amri, R.; Duchemin, B.; Chehbouni, A. Soil texture estimation over a semiarid area using TerraSAR-X radar data. *IEEE Geosci. Remote Sens. Lett.* **2012**, *9*, 353–357.
30. Aubert, M.; Baghdadi, N.; Zribi, M.; Douaoui, A.; Loumagne, C.; Baup, F.; El Hajj, M.; Garrigues, S. Analysis of TerraSAR-X data sensitivity to bare soil moisture, roughness, composition and soil crust. *Remote Sens. Environ.* **2011**, *115*, 1801–1810.
31. Quackenbush, L.J. A review of techniques for extracting linear features from imagery. *Photogram. Eng. Remote Sens.* **2004**, *70*, 1383–1392.
32. Hellwich, O.; Laptev, I.; Mayer, H. Extraction of linear objects from interferometric SAR data. *Int. J. Remote Sen.* **2002**, *23*, 461–475.
33. Chanussot, J.; Mauris, G.; Lambert, P. Fuzzy fusion techniques for linear features detection in multitemporal SAR images. *IEEE Trans. Geosci. Remote Sens.* **1999**, *37*, 1292–1305.
34. Marghany, M.; Hashim, M. Developing adaptive algorithm for automatic detection of geological linear features using RADARSAT-1 SAR data. *Int. J. Phys. Sci.* **2010**, *5*, 2223–2229.
35. Marghany, M.; Sabu, Z.; Hashim, M. Mapping coastal geomorphology changes using synthetic aperture radar data. *Int. J. Phys. Sci.* **2010**, *5*, 1890–1896.
36. Marghany, M. Operational of Canny Algorithm on SAR data for modelling shoreline change. *Photogram. Fernerkundung Geoinf.* **2002**, *2*, 93–102.
37. Ring, U.; Schwartz, H.L.; Bromage, T.G.; Sanaane, C. Kinematic and sedimentological evolution of the Manyara Rift in northern Tanzania, East Africa. *Geol. Mag.* **2005**, *142*, 355–368.
38. Macheyeki, A.S.; Delvaux, D.; Batist, M.D.; Mruma, A. Fault kinematics and tectonic stress in the seismically active Manyara-Dodoma Rift segment in Central Tanzania—Implications for the East African Rift. *J. Afr. Earth Sci.* **2008**, *51*, 163–188.
39. Dawson, J.B. Neogene tectonics and volcanicity in the North Tanzania sector of the Gregory Rift Valley: Contrasts with the Kenya sector. *Tectonophysics* **1992**, *204*, 81–92.
40. Deus, D.; Gloaguen, R.; Krause, P. Water balance modeling in a semi-arid environment with limited *in situ* data using remote sensing in Lake Manyara, East African Rift, Tanzania. *Remote Sens.* **2013**, *5*, 1651–1680.

41. GES DISC (Goddard Earth Sciences (GES) Data and Information Services Center (DISC)). Available online: http://disc.sci.gsfc.nasa.gov/services (accessed on 23 December 2013).
42. Kent, P.E. A note on pleistocene deposits near lake Manyara, Tanganyika. *Geol. Mag.* **1942**, *79*, 72–77.
43. Schwartz, H.; Renne, P.R.; Morgan, L.E.; Wildgoose, M.M.; Lippert, P.C.; Frost, S.R.; Harvati, K.; Schrenk, F.; Saanane, C. Geochronology of the Manyara Beds, northern Tanzania: New tephrostratigraphy, magnetostratigraphy and 40Ar/39Ar ages. *Quatern. Geochronol.* **2012**, *7*, 48–66.
44. Uhlig, C.; Jaeger, F. *Die Ostafrikanische Bruchstufe und die angrenzenden Gebiete zwischen den Seen Magad und Lawa ja Mweri sowie dem Westfuß des Meru*; Mittler: Leipzig, Germany, 1909; p. 63.
45. Jaeger, F. *Das Hochland der Riesenkrater und die umliegenden Hochländer Deutsch-Ostafrikas; 2 Länderkundliche Beschreibung- Band 2*; Mittler: Berlin, Germany, 1913; p. 213.
46. Leakey, L.S.B. East African lakes. *Geogr. J.* **1931**, *77*, 497–508.
47. Dixit, P.C. Pleistocene lacustrine ridged oncolites from the Lake Manyara area, Tanzania, East Africa. *Sediment. Geol.* **1984**, *39*, 53–62.
48. Hillaire-Marcel, C.; Carro, O.; Casanova, J. 14C and ThU dating of Pleistocene and Holocene stromatolites from East African paleolakes. *Quatern. Res.* **1986**, *25*, 312–329.
49. Damnati, B. Sedimentology and geochemistry of lacustrine sequences of the upper Pleistocene and Holocene in intertropical area (Lake Magadi and Green Crater Lake): Paleoclimatic implications. *J. Afr. Earth Sci.* **1993**, *16*, 519–521.
50. Garcin, Y.; Junginger, A.; Melnick, D.; Olago, D.O.; Strecker, M.R.; Trauth, M.H. Late Pleistocene–Holocene rise and collapse of Lake Suguta, northern Kenya Rift. *Quatern. Sci. Rev.* **2009**, *28*, 911–925.
51. Small, D.; Miranda, N.; Meier, E. A Revised Radiometric Normalisation Standard for SAR. In Proceedings of the 2009 IEEE International on Geoscience and Remote Sensing Symposium (IGARSS), Cape Town, South Africa, 12–17 July 2009; pp. 566–569.
52. Infoterra. Radiometric Calibration of TerraSAR-X Data. Available online: http://www.astrium-geo.com/files/pmedia/public/r465_9_tsxx-itd-tn-0049-radiometric_calculations_i1.00.pdf (accessed on 23 December 2013).
53. Lee, J.S. Digital image enhancement and noise filtering by use of local statistics. *IEEE Trans. Pattern Anal. Mach. Intell.* **1980**, *2*, 165–168.
54. Jehle, M.; Perler, D.; Small, D.; Schubert, A.; Meier, E. Estimation of atmospheric path delays in TerraSAR-X data using models *vs.* measurements. *Sensors* **2008**, *8*, 8479–8491.
55. The Scikit-Image Development Team. Scikit-Image-Image Processing in Python, v0.7.2. Available online: http://scikit-image.org/ (accessed on 23 December 2013).
56. Canny, J. A Computational approach to edge detection. *IEEE Trans. Pattern Anal. Mach. Intell.* **1986**, *PAMI-8*, 679–698.
57. Gonzalez, J.H.; Bachmann, M.; Scheiber, R.; Krieger, G. Definition of ICESat selection criteria for their use as height references for TanDEM-X. *IEEE Trans. Geosci. Remote Sens.* **2010**, *48*, 2750–2757.

58. DLR SRTM X-SAR Digital Elevation Models. Status: 2012-09-28. Available online: http://eoweb.dlr.de:8080/eoweb-ng/licenseAgreements/DLR_SRTM_Readme.pdf (accessed on 23 December 2013).
59. Ludwig, R.; Schneider, P. Validation of digital elevation models from SRTM X-SAR for applications in hydrologic modeling. *ISPRS J. Photogram. Remote Sens.* **2006**, *60*, 339–358.
60. Schlüter, T.; Kohring, R. Palaeopathological fish bones from phosphorites of the Lake Manyara area, Northern Tanzania—Fossil evidence of a physiological response to survival in an extreme biocenosis. *Environ. Geochem. Health* **2002**, *24*, 131–140.

© 2014 by the authors; licensee MDPI, Basel, Switzerland. This article is an open access article distributed under the terms and conditions of the Creative Commons Attribution license (http://creativecommons.org/licenses/by/3.0/).